

A relationship between apoptosis and flow during programmed capillary regression is revealed by vital analysis

Annette Meeson, Michelle Palmer, Marcella Calfon and Richard Lang*

Skirball Institute for Biomolecular Medicine, Developmental Genetics Program, Cell Biology and Pathology Departments, New York University Medical Center, 540 First Avenue, New York, NY10016, USA

*Author for correspondence (e-mail: lang@saturn.med.nyu.edu)

SUMMARY

Previous analyses of developmentally programmed capillary regression suggested two distinct causes of vascular endothelial cell (VEC) death. The first appeared to be macrophage-dependent (Lang, R. A. and Bishop, M. J. (1993) *Cell* 74, 453-462) while the second was proposed to result from cessation of blood flow (Lang, R. A., Lustig, M., Francois, F., Sellinger, M. and Plesken, H. (1994). *Development* 120, 3395-3403). Combined, these analyses suggested a model in which initial, macrophage-mediated endothelial cell apoptosis blocked blood flow within a capillary segment and, as a consequence, caused apoptosis of all remaining cells in the affected segment.

In the current study, we have tested this model using a new method that combines vital and histological analyses as a means of determining the fate of whole capillary segments and individual cells *in vivo*. This technique

revealed that one of the first events in regression was the apoptosis of a single VEC in otherwise normal, flowing capillary segments (initiating apoptosis). These isolated, dying VECs projected into and restricted the capillary lumen, imposing either a temporary or permanent block to blood flow. Following cessation of flow, synchronous apoptosis of VECs occurred (secondary apoptosis). In addition, a quantitative analysis revealed a reciprocal relationship between plasma flow and VEC apoptosis. These observations are consistent with a model for capillary regression in which macrophages induce apoptosis in a limited number of VECs and, as a consequence of a block to blood flow, also cause apoptosis in those remaining.

Key words: apoptosis, vascular regression, macrophage, tissue remodelling, tissue regression, rat, capillary regression

INTRODUCTION

Programmed capillary regression is a frequent occurrence in development. Despite the prevalence of this event, and the potential therapeutic value of an understanding of its mechanism, capillary regression is understood at only a rudimentary level. Developmentally programmed capillary involution can be associated with regression of a complex tissue as in the example of the interdigital web (Hurle et al., 1985). In this case, surrounding mesenchymal and ectodermal cells are undergoing programmed death at about the stage of development that capillaries regress. Capillary involution is also associated with differentiative events. This is true for the appearance of avascular regions that arise prior to the condensation of cartilage in the developing digital plate (Feinberg and Noden, 1991). Yet another circumstance is evident in the mammalian eye, where capillaries of the hyaloid system and pupillary membrane undergo regression in the absence of any additional cell death or radical differentiative events (Lang et al., 1994).

A number of models have been proposed to explain the different examples of developmental capillary regression at the cellular level. Induced corneal capillaries have offered an opportunity for analysis of the morphological events associated with regression and have indicated that blood stasis may be a

requirement for the latter stages of regression (Ausprunk et al., 1978). Vessel regression in the precartilaginous regions of the chick foot plate was initially explained based on physical restriction of capillaries when cartilage condensed (Wilson, 1986). This view was lent credence by the observation that a simple physical block to plasma flow would result in the programmed death of vascular endothelial cells (VECs) in the circulation supplying the ovary (Azmi and O'Shae, 1984). Subsequently, definitive marker studies in the chick digital plate indicated that cartilage did not condense until after capillaries had regressed (Hallmann et al., 1987), and the notion that condensation was the key factor was abandoned. The mechanism of capillary regression in the chick digital plate prior to cartilage condensation remains unclear.

A number of electron microscopy studies have examined the morphological changes associated with regression of the hyaloid vessels (Jack, 1972; Balazs et al., 1980; Latker and Kuwabara, 1981; Wang et al., 1990). The presence of macrophages (referred to as hyalocytes or vitreal cells) associated with the hyaloid vessels had been noted (Balazs et al., 1980), though their low number and lack of phagosomes perhaps suggested that macrophages did not play a major role in regression (Latker and Kuwabara, 1981). More recent studies have provided evidence that regression of the capillaries of the pupillary membrane, a structure closely related to the

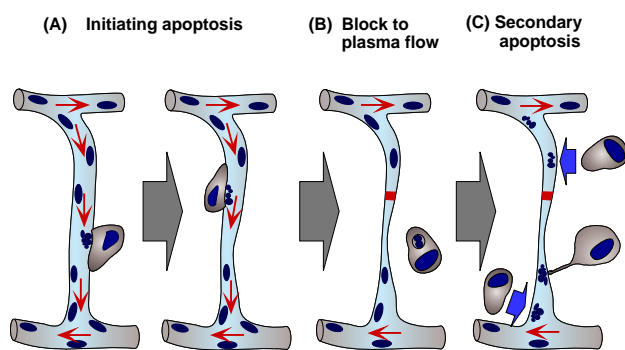


Fig. 1. A model for developmentally programmed capillary regression. Current evidence suggests that programmed capillary regression may occur through a two step mechanism. The model suggests that the first apoptoses of vascular endothelial cells are dependent upon the macrophage (Lang and Bishop, 1993). This event is termed initiating apoptosis (A). We propose that macrophage-mediated VEC death ultimately results in lumen restriction and a block to plasma flow within a capillary segment. Red arrows indicate flow and the red bar, a block to flow (B). We suggest that VECs die subsequently with a synchronous pattern because they are denied survival factors present in plasma. This is referred to as secondary apoptosis (C). The large blue arrows indicate the likely chemotactic response of macrophages to apoptotic cells.

hyaloid system, may be macrophage dependent (Lang and Bishop, 1993). Furthermore, the pattern of programmed cell death during pupillary membrane regression suggests a cellular mechanism to explain the regression process (Lang et al., 1994; Fig. 1). The current model proposes that apoptosis of VECs early in the regression of a capillary segment is macrophage-dependent. These events are discerned histologically as isolated apoptotic VECs in otherwise normal segments and will be referred to as *initiating apoptosis* (Fig. 1A). The model further proposes that initiating apoptosis results in the cessation of plasma flow when the capillary lumen becomes narrow (Fig. 1B). In turn, the model proposes that lack of flow causes the synchronous pattern of apoptosis that has previously been observed, perhaps due to plasma survival factor deprivation (Lang et al., 1994; Fig. 1C). For ease of reference, synchronous apoptosis will be referred to as *secondary apoptosis*.

In the current study, we have combined conventional histological analysis with a new vital cell imaging system to determine when blood flow ceases relative to initiating and secondary apoptosis. We observed that initiating apoptosis preceded and caused flow stasis due to the projection of apoptotic VECs into the capillary lumen. Secondary apoptosis always occurred after blood flow had ceased, arguing that the two events are causally related. In agreement was the reciprocal relationship between plasma flow and VEC apoptosis when these events were quantitated. These observations are consistent with the idea that secondary apoptosis is a consequence of a survival factor deprivation caused by lack of plasma flow.

MATERIALS AND METHODS

Vital cell imaging equipment

Vital cell imaging equipment was centered around a Zeiss Axiophot

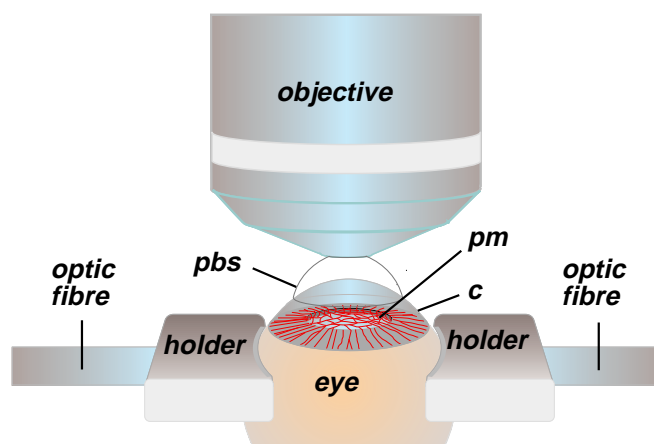


Fig. 2. Vital cell imaging technique. The diagram shows the arrangement of elements for vital cell imaging. A water immersion objective is optically linked to the cornea (c) of an anaesthetized rat with a bead of phosphate-buffered saline (pbs). Axially opposed optic fibre guides deliver light to the orbit and the pupillary membrane (pm). Each light guide is fitted with a curved nylon holder at the tip.

microscope (Zeiss, Thornwood, NY) with custom designed stage plate and long working distance, water immersion objectives. The microscope stage plate was designed to allow coarse micromanipulators to be attached at each side. The manipulators each carry an optic fibre light guide of 1 mm diameter, which has the dual function of illuminating and holding the eye (Fig. 2). Each light guide is fitted with a terminal, nylon eye holder. Oblique illumination with dual, 180° axially opposed light guides was found to give good quality images.

Image recording was provided by a combination of a CCD camera (DXC-760, Sony) and Betacam SP UVW-1400 video recorder (Sony). A Betacam SP PVW-2650 video deck (Sony) was used for its frame search feature and digital images obtained from videotape using a Matrox frame grabber board that was a component of an imaging system combining Metamorph software and a DECpc XL560 computer (Universal Imaging, New York). The presented vital images were generated by combining overlapping, in focus video frames captured as still images. Figures were assembled using Adobe Photoshop and Quark Express software.

Vital cell imaging

Rat pups from postconception (p.c.) day 30.5 to p.c. 34.5 were subdued with metaphane and subsequently anaesthetized with an intramuscular injection of ketamine and xylazine at 1.6 mg/g and 32 mg/g respectively. Depth of anaesthesia was monitored by paw pinch response and where necessary, animals maintained with additional doses of ketamine and xylazine intraperitoneally. The eyelids of rat pups were parted at the suture using microdissecting vannas (Storz, St Louis), the orbit gently raised and the eyelids folded underneath to permit illumination of the eye with optic fibre light guides. The rat pup was then placed in a silastic body mold designed to reduce movement and kept warm with an overlaid heating element from a battery powered boot warmer (L. L. Bean, Maine). The liquid phase for the water immersion objectives was provided by addition of a bead of phosphate-buffered saline between the orbit and objective. Capillaries of the pupillary membrane were readily detected by searching through the focal axis. Regression events in pupillary membranes could be observed for a maximum of about 4 hours. This limit was imposed by a number of factors including reduction of image quality due to gradual opacification of the cornea and sensitivity of the animals to repeated doses of anaesthetic.

Animal breeding

Sprague-Dawley rats were obtained from Taconic Farms (German Town, NY). The age of newborn rats was determined by the presence of sperm in a vaginal fluid smear in the breeding female and the time of conception assigned to the previous midnight. Ages of rats are noted as days postconception (e.g. p.c. 31.5).

Scanning electron microscopy

Scanning electron microscopy was carried out on whole mounts of rat eyes at various stages of development. Whole mounts were prepared by dissecting the retina, sclera, choroid and cornea away from the lens, iris diaphragm, hyaloid vessels and pupillary membrane. The latter tissue group was then fixed overnight in 2% glutaraldehyde in 0.1 M cacodylate pH 7.4, 0.1 M sucrose. After fixation, the tissue was washed in buffer alone and dehydrated in an ethanol series (50%, 70%, 80%, 90%, 95% and 100%). The specimens were then treated for 1 hour in hexamethyldisilazane (Polysciences Inc. Pennsylvania) and then air dried overnight. After drying, they were mounted and sputter coated with approximately 100 angstroms of gold-palladium. Specimens were visualized using a JOEL SEM 840 instrument.

Histological analysis

We have used a modified version of the TUNEL technique (Gavrieli et al., 1992) as previously described (Lang et al., 1994) to identify cells undergoing apoptosis during the regression of the pupillary membrane. The pupillary membrane/iris diaphragm complex was dissected from the rat eye as formerly outlined (Lang et al., 1994). Since the TUNEL technique does not reliably label end-stage apoptotic cells, we have used either TUNEL-labelling or apoptotic morphology revealed by haematoxylin staining as criteria for identifying apoptosis histologically.

In the current study, individual capillary segments visualized vitally were identified in stained preparations using a mapping technique. Briefly, after pupillary membrane imaging, the most rostral point of the cornea was marked with India ink. This served to orient the dissected pupillary membrane preparation relative to the video frame. During dissection, a 'tag' of ciliary body was left attached to the iris diaphragm adjacent to the rostral cornea. Subsequently, TUNEL- or haematoxylin-stained preparations were visualized on a video monitor and compared directly with video tape images obtained vitally. The shape and pattern of capillary branch-points allowed consistent identification of single segments and comparison of vital and histological morphology.

RESULTS

Vital imaging identifies events associated with capillary regression

The morphological changes associated with pupillary membrane regression have been characterised previously at the histological level (Lang et al., 1994) and a temporal sequence of events has been inferred (Fig. 1). In the current study, direct observation of the pupillary membrane during its regression has allowed inferences to be confirmed and has provided a detailed picture of the regression process. Table 1 presents a representative group of capillary segments that were subject to combined vital and histological analysis and for which there was a complete data set. The analysis has been performed with the focus on the flow status of the capillary segments and the number of apoptoses occurring in the different flow classes. Furthermore, in the relevant classes, we have determined whether apoptotic VECs are associated with restricted or blocked blood flow.

The flow categories used in this study, in order of reducing flow status, included (1) free-flowing capillaries (Fig. 3), (2) slow-flowing capillaries (Fig. 8A,B), (3) sporadically flowing capillaries (Fig. 6), (4) capillaries showing plasma flow only (Fig. 8C,D), (5) capillaries showing oscillating movement of contents indicative of a recently established block (Fig. 7), and (6) capillaries without any discernible flow or movement of contents (Fig. 8E,F).

Capillary segments with free flow were recognised based on velocity and number of erythrocytes present. This was also true for slow-flowing capillaries. In vital images presented as still micrographs, reduced flow in a segment is manifest as fewer erythrocytes with discrete rather than blurred outlines (Fig. 8B). Capillaries with sporadic flow occurred with a transient cell-mediated block as described below (Fig. 6). Plasma flow only was observed in some capillaries that had a marked restriction. Flow in these capillaries was discernible due to the passage of small plasma bodies of unknown origin (Fig. 8C,D). Capillaries showing oscillating contents movement were presumed to be recently blocked and, consistent with this assessment, had discrete blocks or short regions of lumen collapse. Oscillating movements were presumably produced with changes in pressure upstream of the block. Capillaries with no discernible flow or movement of contents were presumed to be in the final stage of regression.

Initiating apoptosis occurs in capillaries with plasma flow

In order to determine whether the first apoptotic VECs observed during pupillary membrane regression occur in capillaries with or without plasma flow, we have combined vital and histological analyses as described.

Initiating apoptosis can be identified histologically as isolated TUNEL-labelled VECs in otherwise normal capillary segments. In the example shown (Fig. 3A,B; capillary no. 191-1, Table 1), a TUNEL-labelled apoptotic body was being engulfed by a macrophage (Fig. 3B). Initiating apoptoses like this were discernible *in vivo* as cells in the capillary wall that have convoluted surface topology typical of programmed cell death (Wyllie et al., 1980) (Fig. 5A). Thus, in the corresponding vital image, both apoptosing VECs and macrophages were readily observed (Fig. 3C,D). With good quality histology and vital images, individual cells could be identified. One of the macrophages labelled in Fig. 3B (*m*) was also identifiable in the vital image (Fig. 3D) and had clearly engulfed an apoptotic body (*ap*).

In some examples of initiating apoptosis, deformed VECs projected into the capillary lumen forcing freely flowing white and red blood cells to move around the projection (Fig. 3E,F). Of 26 isolated apoptoses (representing 5.9% of total cells within the examined segments) detected in free-flowing capillaries, 4 (1%) projected into the lumen. Thus, initiating apoptosis was observed in capillaries through which plasma was flowing, an observation consistent with the idea that it represents one of the first events in regression and is independent of flow stasis. Furthermore, the projection of deformed VECs into the capillary lumen suggested that isolated apoptotic events might promote flow stasis.

Macrophages are preferentially associated with initiating apoptosis

Earlier experiments suggest that macrophages may actively

Table 1

		Apoptotic VECs						
Flow category	PM-capillary number	Absolute proportion	Average percentage	At restriction	Summary proportion (%)	Outside restriction	% outside restriction	Nature of block
Free flowing (total <i>n</i> =14)	50-2	5/59	5.9% (26/443)	None	-	5	All, 5.9%	-
	79-3	12/100				12		-
	79-5	1/45				1		-
	103-1	0/17				0		-
	103-2	2/56				2		-
	107-3	3/40				3		-
	119-1	1/45				1		-
	119-3	0/21				0		-
	188-1 ^a	1/40				1		-
	191-1 ^b	1/20				1		-
Sporadic flow (total <i>n</i> =8)	43-1	2/51	27% (43/162)	ND	5/5 (100%)	ND	17%	ND
	43-2	4/11		ND		ND		ND
	82-1	5/22		2		3		Projection of apoptotic bodies
	135-1	18/28		2		16		
	137-1 ^c	8/28		2		6		
	152-1 ^d	5/16		3		2		
	172-1 ^e	1/6		1		0		
Oscillating flow (total <i>n</i> =9)	79-1	48/95	39% (151/384)	2	9/9 (100%)	46	31%	Focal
	118-2	37/102		11		26		Extended
	118-3	3/15		2		1		Focal
	118-4	2/6		2		0		Focal
	119-6	12/45		4		8		Focal
	141-1	21/38		4		17		Focal
	144-1	8/28		2		6		Focal
	172-2 ^f	9/23		3		6		Focal
	189-1	11/32		3		8		Focal
No flow (total <i>n</i> =30)	43-3	6/6	89% (260/292)	-	-	-		Extensive lumen collapse
	82-4	15/15		-	-	-		
	98-1	10/10		-	-	-		
	99-3	14/16		-	-	-		
	103-7	38/50		-	-	-		
	103-8	29/35		-	-	-		
	105-1	53/60		-	-	-		
	107-1	12/13		-	-	-		
	107-2	38/38		-	-	-		
	108-1	5/6		-	-	-		
	109-1	6/6		-	-	-		
	122-1	9/10		-	-	-		
	152-2	25/27		-	-	-		

^aFree flowing capillary segment shown in Fig. 3E and F.

^bFree flowing capillary segment shown in Fig. 3A-D.

^cSporadically flowing capillary shown in Fig. 6A-C.

^dSporadically flowing capillary shown in Fig. 6D-G.

^eSporadically flowing capillary shown in Fig. 7A and B. This capillary segment display temporary and permanent blocks to flow during the course of the observational period.

^fOscillating flow capillary shown in Fig. 7C and D.

a-f: Complete capillary segments are not always shown in the figure panels.

induce death of VECs during regression of the pupillary membrane (Lang and Bishop, 1993). Given the additional requirement that macrophages and target cells are in close contact in an induction of apoptosis (Aliprantis et al., 1996), it follows that macrophages should be found preferentially associated with initiating apoptosis.

To examine this issue, we measured, in stained preparations, the distance from isolated apoptotic VECs to the nearest macrophage (Fig. 4). For controls, we determined the distance from the nearest macrophage to apoptotic VECs in secondary apoptosis and to randomly chosen normal VECs. Macrophages were in direct contact with initiating apoptosis in 22 out of 38 examples. By contrast, macrophages were, on average, further

from VECs undergoing secondary apoptosis and most distant from randomly chosen normal VECs. These data indicate that macrophages have a special association with VECs that are undergoing apoptosis.

The distances measured between apoptotic VECs and macrophages (Fig. 4) may have been overestimated since macrophages extended pseudopodia over many cell diameters toward apoptotic VECs (Fig. 5A). Macrophage pseudopodia were also observed in samples prepared for scanning electron microscopy (Fig. 5B). Pseudopodia such as these were not readily observed in the histological preparations in which macrophage-to-VEC distance was measured, leading to a minor but systematic overestimate of macrophage-to-VEC distance.

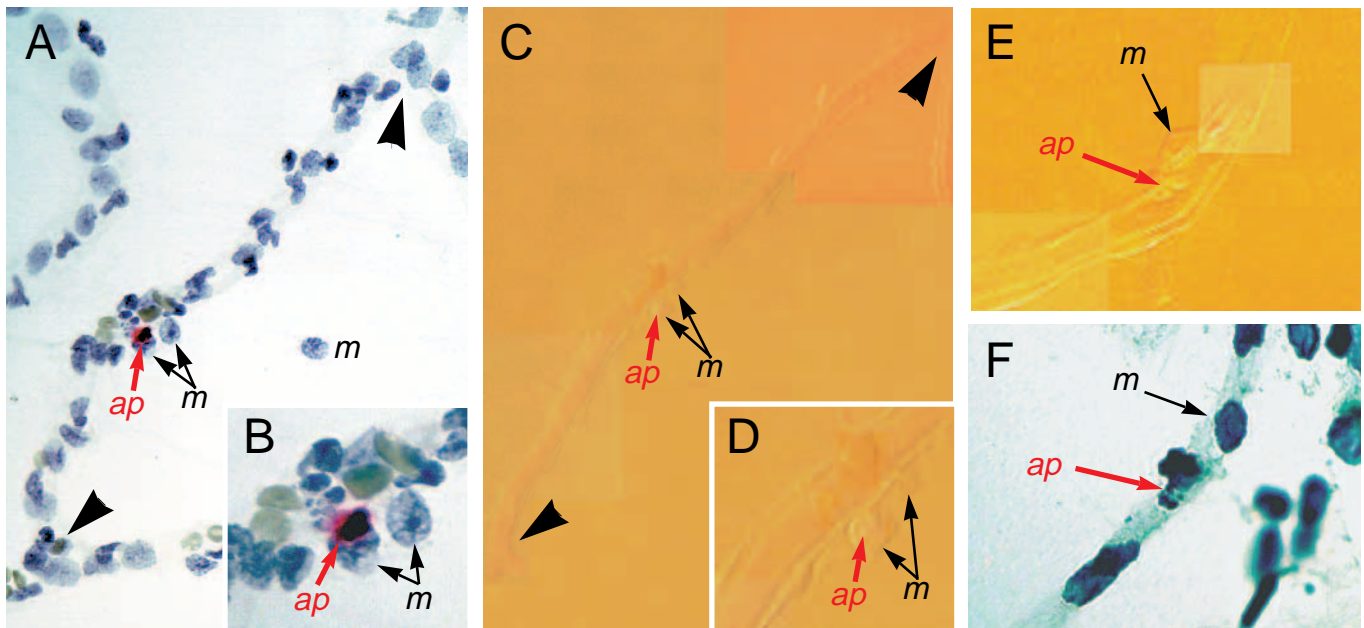


Fig. 3. Initiating apoptosis in the pupillary membrane. (A) Initiating apoptosis is shown as a TUNEL-labelled apoptotic cell (*ap*) in an otherwise normal capillary. Three macrophages are indicated (*m*) and capillary branch-points are marked by large arrowheads (400 \times). (B) At higher magnification, an apoptotic body (*ap*) is observed being engulfed by a macrophage (*m*). In vital images of the same capillary segment (C,D) the apoptotic endothelial cell (*ap*) and accompanying macrophages (*m*) are readily observed (C, 400 \times ; D, 800 \times). Vital observations of another rat pupillary membrane at day 33.5 p.c. shows an initiating apoptotic event (*ap*) in which a deformed VEC can be seen projecting into the capillary lumen. A macrophage (*m*) is positioned on the non-luminal surface of the capillary in close proximity to the apoptosis (E) (800 \times). This event is also identified histologically with morphology typical of apoptosis (F) (800 \times). Magnifications are given in brackets.

Extracellular matrix fibres are associated with the capillaries of the pupillary membrane and were readily observed in scanning electron micrographs (Fig. 5B). The matrix fibres regress along with remaining components and regress from the central region of the pupillary membrane first (data not shown). In addition, during vital observation, we occasionally observed erythrocytes escaping in small numbers from the lumen of flowing capillaries. The erythrocytes appeared to be extruded through small holes in the capillary wall as evidenced by their dumbbell shape upon exit or entrapment. These events can be visualized both vitally (Fig. 5C) and histologically (data not shown) and indicate that the basal lamina of capillaries can be discontinuous.

Discrete blocks to plasma flow occur adjacent to initiating apoptoses

In order to determine whether initiating apoptosis could cause cessation of plasma flow, we assessed individual capillary segments that were making the transition from flow to stasis. Capillary segments showing this characteristic were rare and this is presumably an indication of the relative transience of this condition. Capillary segments examined vitally were identified in histological preparations using the mapping technique described in Materials and Methods.

The transition from flow to stasis in a capillary segment occurs when a formerly moving cell becomes trapped where the capillary lumen is narrow, a condition that is invariably associated with VEC apoptosis. Of 14 sporadic or oscillating flow capillaries for which there was complete data, 100% showed apoptotic VECs at the point of restriction (Table 1, column 6).

Some blocks to flow were temporary (sporadic flow). This occurred when a white or red blood cell wedged into a

narrowed region of the lumen adjacent to an apoptotic cell, progressed slowly past the restriction, and then proceeded freely (Fig. 6A-C; capillary number 137-1, Table 1). In some examples, cells wedged into a narrow lumen were trapped for an extended period of time (Fig. 6D-G; capillary number 152-

Macrophage to endothelial cell distance

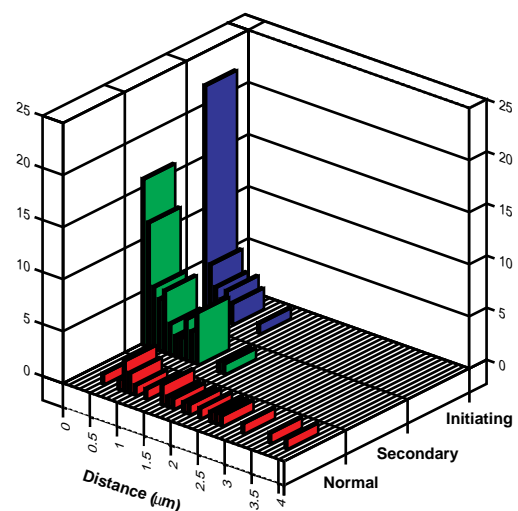


Fig. 4. Macrophages are preferentially associated with apoptosing cells. Chart representing the endothelial cell to macrophage distance (in μm) for initiating apoptosis, secondary apoptosis and as a control, randomly chosen, non-apoptotic endothelial cells. In all cases counts were taken from day 33.5 p.c. rat pupillary membranes.

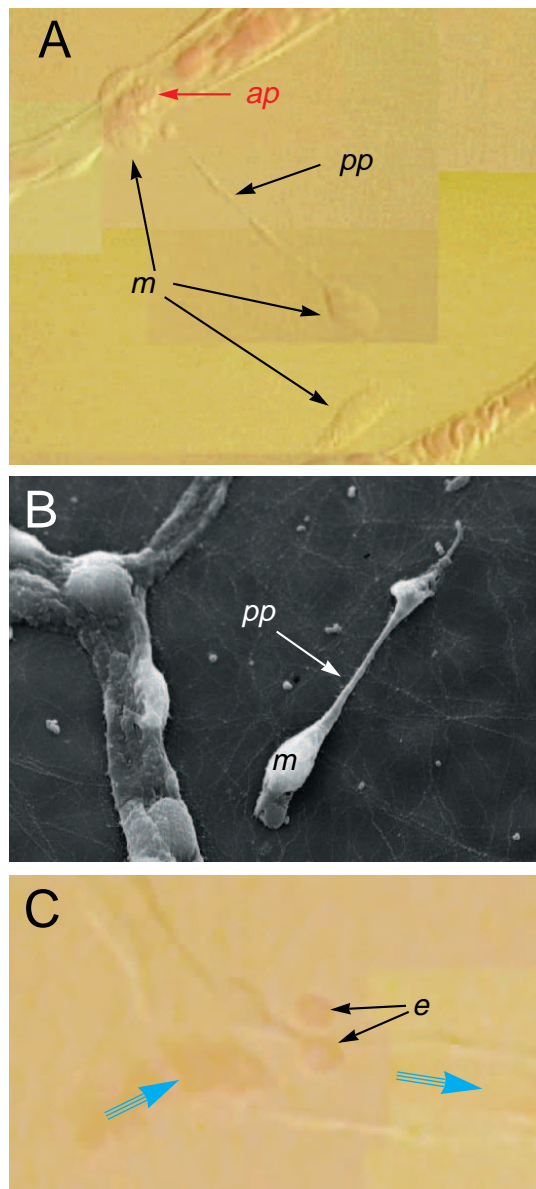


Fig. 5. Macrophages make cell-cell contact over large distances. (A) Vital cell image of macrophage (*m*) with extended pseudopod (*pp*) in which the pseudopod was in contact with an apoptotic cell (*ap*). Additional macrophages, one of which is in contact with the apoptosis, are indicated (*m*, arrows) (800 \times). (B) Scanning EM image of whole mount pupillary membranes also revealed the presence of macrophages (*m*) with extended pseudopodia (*pp*). Extracellular matrix fibres that are part of the pupillary membrane can be seen resting on the anterior surface of the lens capsule (800 \times). (C) Erythrocyte (*e*) partially extruded through the wall of a capillary. The erythrocyte has adopted a dumbbell shape. The blue arrows indicate the direction of flow at a branch-point (900 \times). Magnifications are given in brackets.

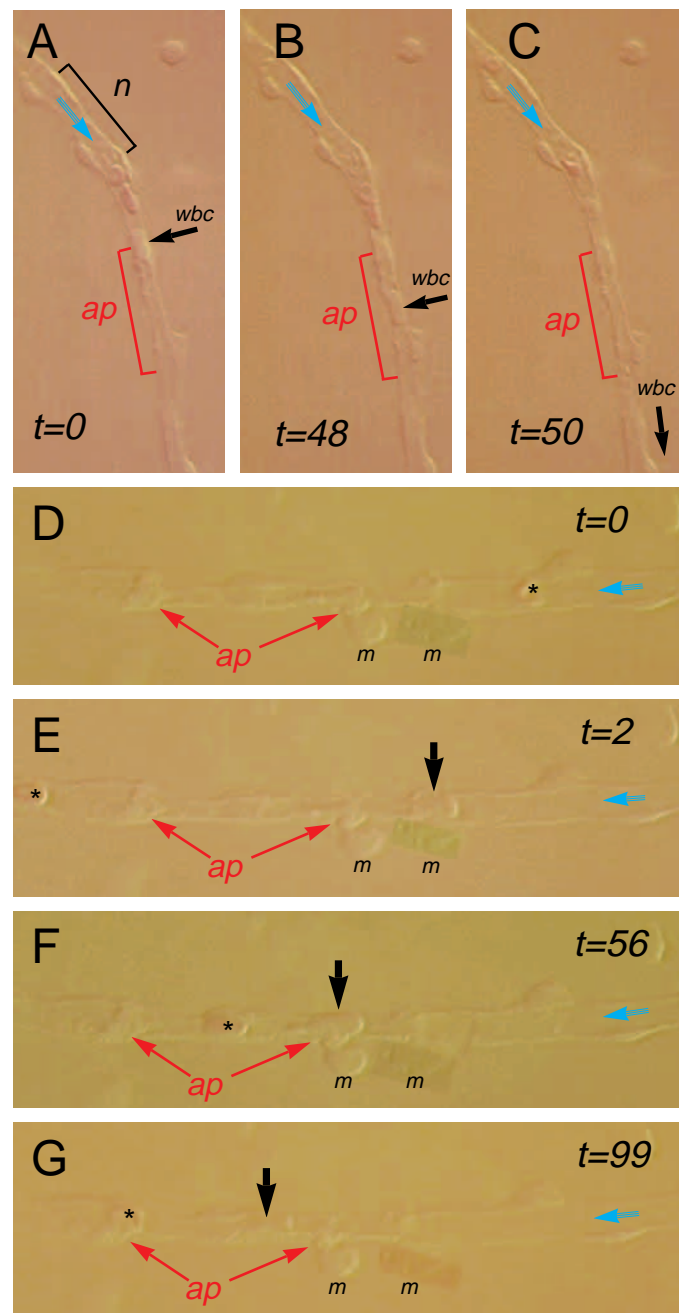


Fig. 6. Apoptoses cause lumen restrictions and sporadic blocks to flow. (A-C) Vital cell images of a day 32.5 p.c. capillary segment in which a block to flow is caused by trapping of a white blood cell (*wbc*, black arrow) in a narrowed region of the capillary. In this region, the VEC shows membrane undulations indicative of apoptotic changes (*ap*). These can be compared with a normal region of the capillary wall (*n*). The direction of flow is indicated by blue arrows and the time (*t*) elapsed between frames is indicated in seconds. (D-G) A similar situation is seen in another pupillary membrane at day 33.5 p.c. but in this case, a temporary block is caused by the trapping of a red blood cell (black arrow) in a region where two VECs are apoptotic (*ap*). Macrophages (*m*) are seen associated with apoptoses. An additional red blood cell that moves against the direction of flow after the block is established is indicated by an asterisk. All magnifications are 400 \times .

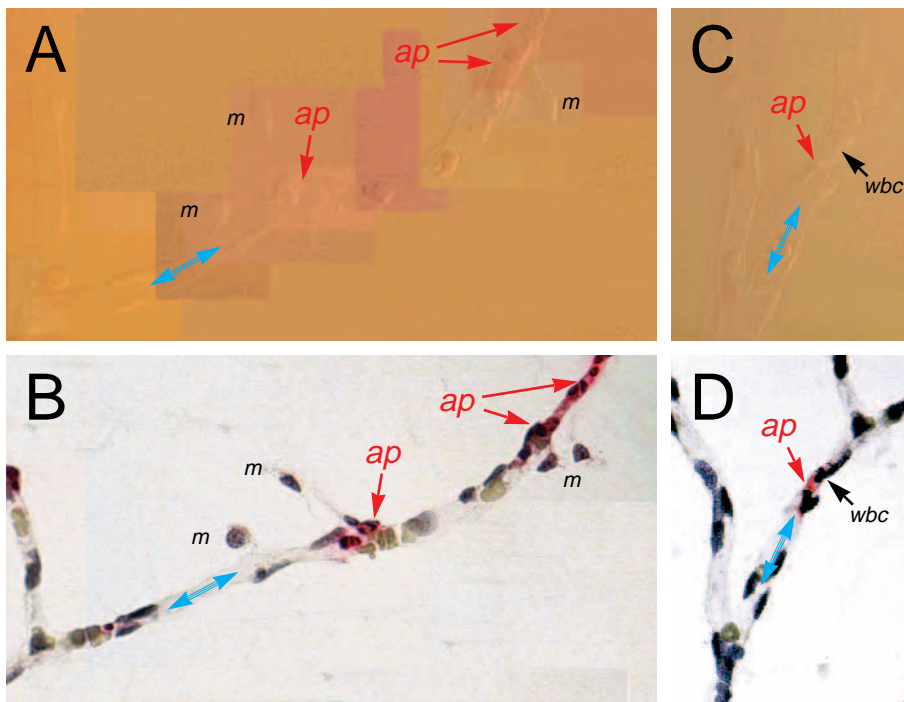


Fig. 7. Apoptoses cause permanent blocks to blood flow. (A) Vital image of day 33.5 p.c. capillary segment in which flow has ceased and oscillating movement of erythrocytes is apparent. Apoptotic morphology is observed at two locations within the segment (*ap*). The uppermost example of apoptotic morphology is associated with a collapsed region of the segment and is probably the cause of the block to flow. Multiple macrophages are associated with the apoptoses (*m*). Oscillating flow is indicated by double-headed blue arrows. (B) The corresponding histological preparation shows apoptoses as red TUNEL-labelled areas (*ap*). Macrophages (*m*) are also observed in the bright-field image. (C) Vital image of capillary segment in which a white blood cell (*wbc*) has become lodged in the lumen adjacent to an apoptotic VEC (*ap*). (D) Corresponding bright-field image showing TUNEL-labelled cell and the probable nucleus of the trapped white blood cell (*wbc*). All magnifications are 400 \times .

1, Table 1) and ultimately, we presume, caused a permanent block to flow. Apoptotic morphology was discernible as subtle undulations in the capillary wall that contrasted with the smooth surface of normal cells (compare normal VEC (*n*) with apoptotic VEC (*ap*) in Fig. 6A-C). In other instances, apoptosis is more obvious due to the projection of apoptotic blebs into the capillary lumen (Figs 3E, 6D-G).

Where flow stasis appeared permanent by vital observation, apoptosis of VECs could be documented at the point of restriction with TUNEL labelling (Fig. 7). Capillaries were presumed to have a recently established block when erythrocytes within the lumen were oscillating. The presence of an apoptotic event adjacent to a block observed vitally was confirmed using either TUNEL labelling or hematoxylin staining in a histological preparation and in some cases, red blood cells were observed oscillating upstream of the block (compare Fig. 7A with B; capillary number 172-1, Table 1).

In others, white blood cells that were seen to cause a block during vital observation could be confirmed as adjacent to an apoptosis in TUNEL-labelled histological preparations. Capillary number 172-1 (Fig. 7C,D) is of particular interest since during the course of vital observation, a number of white blood cells became trapped adjacent to an irregularity in the luminal wall and induced an oscillating movement of capillary contents. White cell trapping was repeated a number of times until the end of the observational period. The luminal projection was found to be an apoptotic VEC upon TUNEL labelling of a histological preparation (Fig. 7D). Given that a cell-mediated block occurred in 5/5 sporadic flow capillaries observed, we presume that this represents the predominant mechanism by which blood stasis occurs.

The question of whether initiating apoptosis always precedes secondary apoptosis is answered through examination of the percentage of apoptotic VECs found in capillaries that are making the transition from flow to stasis. For capillaries

displaying free flow or sporadic flow, the number of apoptotic VECs is 5.9% and 27% respectively. This means that 1 in 17 (free flow) or approximately 1 in 4 (sporadic flow) VECs are undergoing apoptosis at any one time. Given that any histological assessment is only a snapshot in time, it is very likely that isolated apoptosis will be occurring continually for a period of time prior to the appearance of secondary apoptosis.

Secondary VEC apoptosis occurs after plasma flow has ceased

To extend our conclusions from observation of individual capillary segments, the overall relationship between flow status and apoptosis was quantitated. For this purpose, we compared vital and TUNEL images for a series of capillaries in different states of flow. Since there was short-term variation in flow rate through any one segment, it was not meaningful to directly quantitate flow rate. Instead, capillary segments were grouped into one of six categories relevant to flow status that were easily distinguished from one another during vital observation (see beginning of results for definitions). Once segments of interest had been identified vitally, pupillary membranes were removed, subject to TUNEL analysis, and the capillary of interest located. Total and apoptotic VECs within the segment were counted and the proportion of apoptotic cells expressed as a percentage. The average was calculated for each group (Fig. 9; Table 1) and shows that, as flow diminished, the proportion of apoptotic cells increased. This is consistent with the notion that reduced or completely blocked flow may be the cause of secondary apoptosis in a capillary segment.

DISCUSSION

Programmed capillary regression is a frequently occurring but poorly understood aspect of development. The subject of the

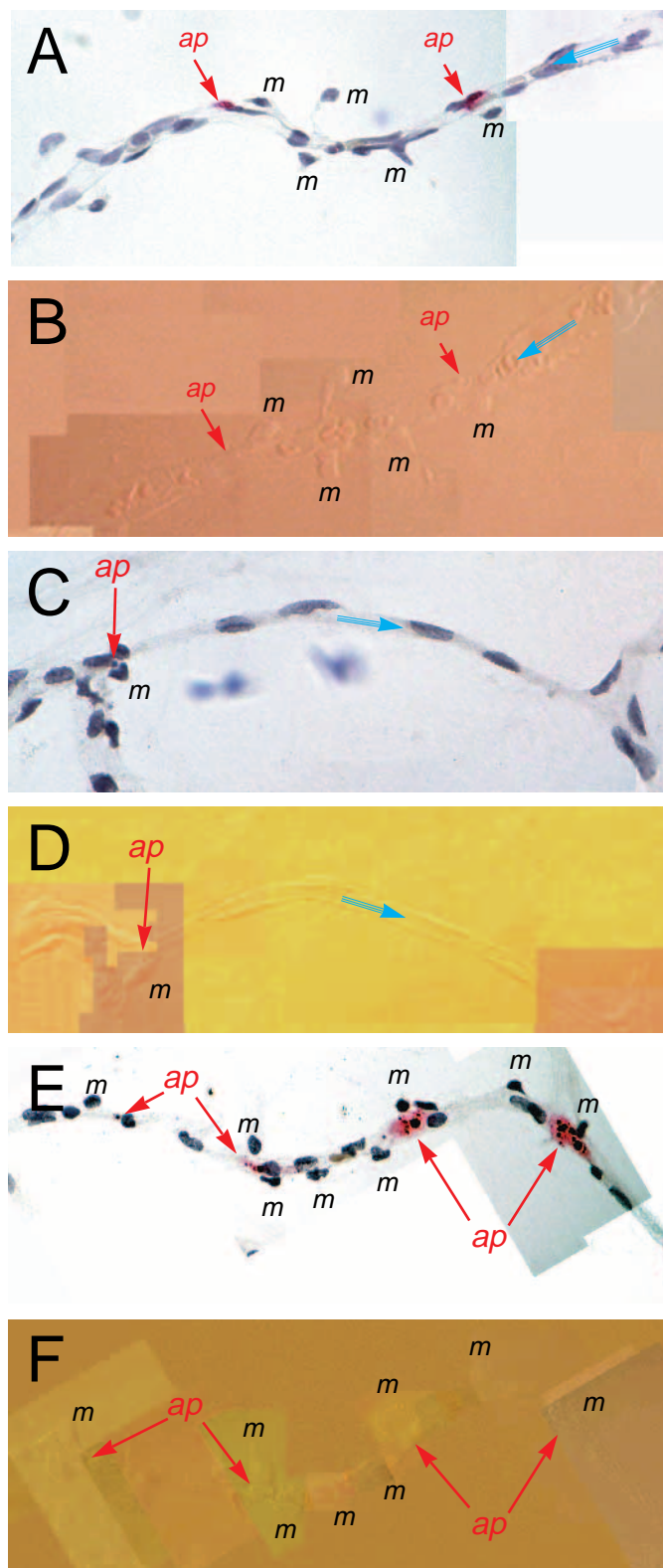


Fig. 8. Appearance of capillaries in various states of flow.

(A) Histological and TUNEL-labelled preparation of a capillary that vitally (B) was identified as having slowed blood flow. This was apparent from a reduced number of erythrocytes with discrete outlines. Two apoptotic cells (*ap*) are present within this capillary segment and several macrophages (*m*) are in direct contact with this capillary. (C) Bright-field image of a short capillary segment that showed plasma flow only in vital observation. A macrophage (*m*) and an adjacent apoptotic cell (*ap*) located at one capillary junction are indicated. (D) The same capillary segment as in (C) shown vitally. No erythrocytes are apparent in the segment and the direction of flow is indicated by the blue arrow. (E) Bright-field image of a capillary with multiple, TUNEL-labelled apoptoses (*ap*) that vitally (F) was observed to have no flow. Individual macrophages are readily identified in both bright-field and vital images (*m*). All magnifications are 400 \times .

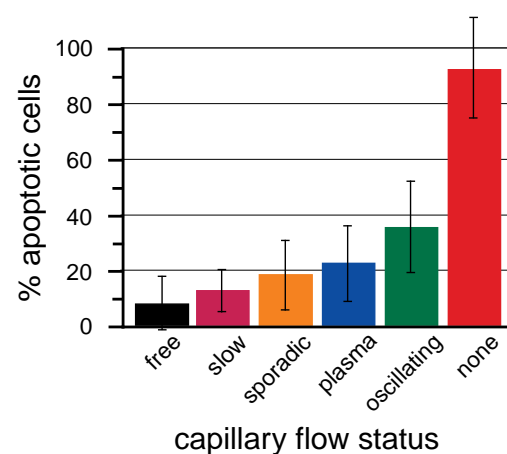


Fig. 9. Relationship between capillary flow and VEC apoptosis. Bar chart representing the percentage of apoptotic cells within capillary segments, compared with flow status (day 33.5 p.c. animals).

Capillaries were divided into one of six categories depending on their blood flow status observed vitally (refer to text). The capillaries were subjected to TUNEL analysis and the number of apoptotic cells counted. The average number of apoptoses was determined for each group and expressed as a percentage.

1993) or of cessation of blood flow (Lang et al., 1994). In this study, we have examined the role that plasma flow may play in capillary regression and determined whether events inferred from histological analysis occur in vivo. To this end, a vital cell imaging technique was developed and combined with conventional histological analysis to further probe the mechanism of capillary regression.

The suggestion that macrophages are actively involved in the induction of VEC apoptosis is based on the observation that, in transgenic mice with limited macrophage function, the pupillary membrane was seen to persist in viable form (Lang and Bishop, 1993). Though not conclusive when viewed in isolation, the observation that macrophages are preferentially associated with initiating apoptosis is consistent with the possibility that macrophages induce apoptosis (assuming killing requires contact (Aliprantis et al., 1996)). Other explanations for this association include the action of a macrophage chemotaxin after VECs are committed to apoptosis. This possibility is certainly more likely for secondary apoptosis where there are compelling reasons to believe that VEC death may be a

current analysis, the pupillary membrane, is one example of a capillary network that regresses in a developmentally programmed manner. Our previous analysis of pupillary membrane regression suggests that VEC apoptosis is a consequence either of direct macrophage action (Lang and Bishop,

consequence of plasma stasis. Initiating apoptosis occurs in capillaries that retain vigorous flow and this excludes the possibility that all VEC apoptosis is due to stasis.

The current model proposes that, directly or indirectly, macrophages drive all aspects of programmed capillary regression. This necessarily implies that there is a link between macrophage-induced apoptosis and the flow stasis that is proposed to result in secondary apoptosis. This connection is made by the observation that apoptotic VECs project into the lumen of capillaries that are flowing normally and cause a restriction. In some cases, it is clear that apoptotic VECs can rapidly impose stasis by trapping white or red blood cells in the capillary lumen.

Azmi and O'Shae (1984) have documented that when there is a mechanical block to blood flow, the consequence is apoptosis of VECs within the involved capillaries. These observations are important in the context of the current experiments, since they suggest a cause for the synchronous pattern of secondary apoptosis. Thus, indirectly, macrophages may cause secondary apoptosis through the shape changes induced in VECs undergoing initiating apoptosis.

Although all temporary or permanent flow restrictions are associated with apoptotic VECs, the converse is not true. It is clear (Table 1; Fig. 9) that some apoptotic VECs are found in capillaries that were still flowing freely (5.9% of total cells, on average) while those capillaries undergoing the transition from flow to stasis showed some apoptotic VECs that were not associated with the point of restriction (Table 1; sporadic flow, 17%; oscillating flow, 31%).

There presumably exists a complex relationship determining the number of apoptoses required to establish a block in any given capillary. This will be influenced by the diameter of the capillary, the density with which cells are packed in the endothelium, the pressure that produces flow and the relative location of multiple apoptotic events. It is not surprising that a single apoptotic VEC has little impact on flow in all but the smallest capillaries. It is likely, as the model suggests (Fig. 1), that there is a period of time where macrophage-induced apoptosis has a minimal overall impact on capillary regression. Presumably though, macrophages will eventually produce a threshold proportion of apoptotic VECs critical to the imposition of a block. Indeed, the data suggest that 5.8% apoptotic VECs is, on average, insufficient to produce a block (i.e. free-flowing capillaries) but that 27% (i.e. sporadic flow capillaries) or a greater proportion is, on average, sufficient to cause a block.

Quantitative analysis of many capillary segments indicates that as the blood flow in a capillary segment is diminished, the percentage of cells undergoing apoptosis increases (Fig. 9; Table 1). This suggests that, for the second phase of regression, the two phenomena are interrelated. We have previously suggested that if there were survival factors for VECs present in neonatal plasma, a block to plasma flow would effectively deprive all cells within one segment of the stimulus (Lang et al., 1994). This can explain why regression is segmental and why apoptosis is finally observed to occur synchronously within a segment. Thus, one explanation for the relationship between death and flow is that the level of survival factor to which VECs within a segment are being exposed is being reduced in proportion with reducing flow. Our observations suggest that some cells within a segment may undergo

apoptosis as a result of survival factor deprivation as flow is reducing, but that ultimately, there is a catastrophic induction of apoptosis when flow is stopped completely.

Also interesting is the recent observation that, in the abnormal regression of retinal capillaries (due to conditions of hyperoxia), vascular endothelial cell growth factor (VEGF) acts as a survival factor and can prevent the apoptosis associated with regression (Alon et al., 1995). As a consequence, the soluble VEGF isoforms must be considered prime candidates for circulating survival stimuli that, when withdrawn, would cause the observed secondary apoptosis within the pupillary membrane.

While growth factor deprivation induced apoptosis is an appealingly simple way to explain secondary apoptosis during programmed capillary regression, it is likely that there is a more complex relationship between blood flow and apoptosis. It has long been recognised that oxygen availability influences cell survival and it is possible that reduced blood flow in the capillaries of the pupillary membrane could result in hypoxia. It is clear that expression of a number of growth factors that might influence VEC survival is modulated by hypoxia (Shweiki et al., 1992; Kuwabara et al., 1995; Brogi et al., 1996). Furthermore, the expression of some growth factors genes is modulated by shear force (Malek et al., 1993; Resnick and Gimbrone, 1995) and this, too, may have implications for regression of the pupillary membrane where flow cessation appears to play an important role.

In an extension of the current model explaining programmed capillary regression, it is possible that where complex tissues regress, the process is driven by vascular involution. The interdigital region, for example, is richly supplied with vasculature prior to its regression (Feinberg and Saunders, 1982; Feinberg et al., 1986) and one can suggest that a controlled involution of the vasculature supporting the mesenchymal and ectodermal components might result in the observed apoptosis (Zou and Niswander, 1996) also due, perhaps, to growth factor deprivation. Certainly, evidence is rapidly accumulating that all cell populations are dependent upon survival factors in vivo (Angeletti et al., 1971; Raff, 1992; Chow et al., 1995; Campochiaro et al., 1996). Our future experiments are aimed at further delineating the mechanistic possibilities.

We are particularly grateful to Jon Weider and Joshua Hart for assistance with all aspects of imaging and computer systems and to Edith Robbins and Owen Meyers for training M. P. in scanning EM technique. We would like to thank Titia de Lange for comment on the manuscript. This work was supported in part by development funds from the Kaplan Comprehensive Cancer Center at NYU and by NIH RO1 grants EY10559-01 and EY11234-01 from the National Eye Institute (R. A. L.). In addition, we acknowledge research support for the laboratory of R. A. L. from The Searle Scholars Program of the Chicago Community Trust.

REFERENCES

- Aliprantis, A. O., Diez Roux, G., Mulder, L., Zychlinsky, A. and Lang, R. A. (1996). Do macrophages kill through apoptosis? *Immunology Today* In press.
- Alon, T., Hemo, I., Itin, A., Pe'er, J., Stone, J. and Keshet, E. (1995). Vascular endothelial growth factor acts as a survival factor for newly formed retinal vessels and has implications for retinopathy of prematurity. *Nature Medicine* 1, 1024-1028.

- Angeletti, P. U., Levi-Montalcini, R. and Caramia, F.** (1971). Analysis of the effects of the antiserum to the nerve growth factor in adult mice. *Brain Research* **27**, 343-355.
- Ausprunk, D. H., Falterman, K. and Folkman, J.** (1978). The sequence of Events in the Regression of Corneal Capillaries. *Lab. Investigation* **38**, 284-294.
- Azmi, T. I. and O'Shae, J. D.** (1984). Mechanism of deletion of endothelial cells during regression of the corpus luteum. *Lab. Investigation* **51**, 206-217.
- Balazs, E. A., Toth, L. Z. and Ozanics, V.** (1980). Cytological studies on the developing vitreous as related to the hyaloid vessel system. *Albrecht v. Graefes Arch. klin. exp. Ophthalm.* **213**, 71-85.
- Brogi, E., Schattelman, G., Wu, T., Kim, E. A., Varticovski, L., Keyt, B. and Isner, J. M.** (1996). Hypoxia-induced paracrine regulation of vascular endothelial growth factor receptor expression. *J. Clin. Invest.* **97**, 469-476.
- Campochiaro, P. A., Chang, M., Ohsato, M., Vinore, S. A., Nie, Z., Hjelmeland, L., Mansukhani, A., Basilico, C. and Zack, D.** (1996). Retinal degeneration in transgenic mice with photoreceptor-specific expression of a dominant-negative fibroblast growth factor receptor. *J. Neuroscience* **16**, 1679-1688.
- Chow, R., Diez Roux, G., Roghani, M., Palmer, M., Rifkin, D. B., Moscatelli, D. A. and Lang, R. A.** (1995). FGF suppresses apoptosis and induces differentiation of fibre cells in the mouse lens. *Development* **121**, 4383-4393.
- Feinberg, R. and Noden, D.** (1991). Experimental analysis of blood vessel development on the avian wing bud. *Anatomical Record* **231**, 136-144.
- Feinberg, R. and Saunders, J.** (1982). Effects of excising the apical ectodermal ridge on the development of the marginal vasculature of the wing bud in the chick embryo. *J. Exp. Zoology* **219**, 345-354.
- Feinberg, R. N., Latker, C. H. and Beebe, D. C.** (1986). Localized vascular regression during limb morphogenesis in the chicken embryo. I. Spatial and temporal changes in the vascular pattern. *Anatomical Record* **211**, 405-409.
- Gavrieli, Y., Sherman, Y. and Ben-Sasson, S. A.** (1992). Identification of programmed cell death in situ via specific labeling of nuclear DNA fragmentation. *J. Cell. Biol.* **119**, 493-501.
- Hallmann, R., Feinberg, R., Latker, C., Sasse, J. and Risau, W.** (1987). Regression of blood vessels precedes cartilage differentiation during chick limb development. *Differentiation* **34**, 98-105.
- Jack, R. L.** (1972). Regression of the hyaloid vascular system: An ultrastructural analysis. *Am. J. Ophthalm.* **74**, 261-272.
- Kuwabara, K., Ogawa, S., Matusumoto, M., Koga, S., Clauss, M., Pinsky, D. J., Lyn, P., Leavy, J., Witte, L., Joseph-Silverstein, J., Furie, M. B., Torcia, B., Cozzolino, F., Kamada, T. and Stern, D. M.** (1995). Hypoxia-mediated induction of acidic/basic fibroblast growth factor and platelet-derived growth factor in mononuclear phagocytes stimulates growth of hypoxic endothelial cells. *Proc. Natl. Acad. Sci. USA* **92**, 4606-4610.
- Lang, R. A. and Bishop, M. J.** (1993). Macrophages are required for cell death and tissue remodeling in the developing mouse eye. *Cell* **74**, 453-462.
- Lang, R. A., Lustig, M., Francois, F., Sellinger, M. and Plesken, H.** (1994). Apoptosis during macrophage-dependent tissue remodelling. *Development* **120**, 3395-3403.
- Latker, C. H. and Kuwabara, T.** (1981). Regression of the tunica vasculosa lentis in the postnatal rat. *Ophthalmol. Vis. Sci.* **689**-699.
- Malek, A. M., Gibbons, G. H., Dzau, V. J. and Izumo, S.** (1993). Fluid Shear Stress Differentially Modulates Expression of Genes Encoding Basic Fibroblast Growth Factor and Platelet-derived Growth Factor B Chain in Vascular Endothelium. *J. Clin. Invest.* **92**, 2013-2021.
- Raff, M. C.** (1992). Social controls on cell survival and cell death. *Science* **256**, 397-400.
- Resnick, N. and Gimbrone, M. A.** (1995). Hemodynamic forces are complex regulators of endothelial gene expression. *FASEB J.* **9**, 874-882.
- Shweiki, D., Itin, A., Soffer, C. and Keshet, E.** (1992). Vascular endothelial growth factor induced by hypoxia may mediate hypoxia-initiated angiogenesis. *Nature* **359**, 843-845.
- Wang, J.-L., Toida, K. and Uehara, Y.** (1990). The tunica vasculosa lentis; An expedient system for studying vascular formation and regression. *J. Electron Microsc.* **39**, 46-49.
- Wilson, D. J.** (1986). Development of avascularity during cartilage differentiation in the embryonic limb. *Differentiation* **30**, 183-187.
- Wyllie, A. H., Kerr, J. F. R. and Currie, A. R.** (1980). Cell death: The significance of apoptosis. *Int. Rev. Cytol.* **68**, 251-305.
- Zou, H. and Niswander, L.** (1996). Requirement for BMP signalling in interdigital apoptosis and scale formation. *Science* **272**, 738-741.

(Accepted 18 September 1996)